

## **Electrochemical Synthesis of NiAu Bimetallic Nanostrips and Their Application for Hydrazine Detection**

*Lin-Lin Hou, Ye Wan, Jia-Yin Li, Jun-Rui Zhang, Keying Cui, Su-Juan Li\**

Henan Province Key Laboratory of New Optoelectronic Functional Materials, College of Chemistry and Chemical Engineering, Anyang Normal University, Anyang, 455000, Henan, China

\*E-mail: [lemontree88@163.com](mailto:lemontree88@163.com)

*Received:* 13 February 2019 / *Accepted:* 28 March 2019 / *Published:* 10 May 2019

---

NiAu bimetallic nanostrips with nearly monodispersed structure were synthesized through a one-step electrodeposition method with cetyltrimethylammonium bromide (CTAB) involved as the stabilizer and  $\text{Ni}(\text{NO}_3)_2$  and  $\text{HAuCl}_4$  with a molar ration of 1:1 as the precursor. The morphology of as-prepared NiAu bimetallic nanomaterials with different Ni/Au molar ratios were characterized with scanning electron microscopy (SEM). The resultant NiAu bimetallic nanostrips showed good electrocatalytic activities toward hydrazine oxidation. Various parameters including Ni/Au molar ratios, CTAB concentration and solution pH affecting the performance of NiAu bimetallic nanomaterials toward hydrazine detection were investigated. Under optimized conditions, NiAu bimetallic nanostrips based electrochemical hydrazine sensor has a linear response in the concentration range of 0.5 to 1665  $\mu\text{M}$ , a lower detection limit of 0.1  $\mu\text{M}$  and high detection sensitivity ( $1007 \mu\text{A mM}^{-1} \text{cm}^{-2}$ ). Most common ions and many environmental organic species do not interfere with the detection of hydrazine.

---

**Keywords:** Bimetallic nanostrip; Electrodeposition; Hydrazine; Nickle; Gold

### **1. INTRODUCTION**

The sensitive determination of hydrazine is practically important as it is intensively applied in many areas, such as fuel cells and rocket propellants, chemical and agricultural industry, pharmaceutical intermediates, and other fields including insecticides, explosives, and so on [1-4]. However, hydrazine is toxic and have adverse health effects to the human body when exposure to the air containing 10 ppb hydrazine[5,6]. Therefore, it is highly desirable to develop sensitive and reliable methods for the quantification of hydrazine. Among the various reported methods [7-14], electrochemical oxidation and detection of hydrazine have arised considerable interest owing to its cost-effectiveness, convenient operation, high sensitivity and ease of miniaturization [15-17]. In a common hydrazine electrochemical sensor, the electrocatalytic oxidation kinetics of hydrazine on electrode surface play a significant role in determining its detection sensitivity and selectivity.

Therefore, developing materials which can electrocatalyze hydrazine with large oxidation current and low overpotential is urgently required.

Au nanomaterials have been proved to show excellent electrocatalytic activities towards hydrazine oxidation [6,13]. However, its relatively high cost and scarce reserve of such precious metal becomes a limitation in using it for the fabrication of electrode. As a result, attempts on reducing Au usage with a minimal amount and meanwhile increasing electrocatalytic sites of Au as much as possible is of great concern in developing novel Au-based catalysts for analytical sensors. An efficient strategy include introducing cheap metals in the Au-based catalyst and constituting a multimetallic Au-based catalysts with designed shapes and compositions [18-20], while enhancing the whole electrocatalytic activity and thus its sensing performance toward target species. Nickel (Ni), as a transition metal, has been considered to have similar electrocatalytic activity to Au and could replace the noble metal in some electrochemical sensors. Ni nanostructures show superior catalytic performance toward electro-oxidation of hydrazine, but the catalysis takes place at strong alkaline conditions [21]. Therefore, compared to monometallic Au-based devices, introduction of Ni into Au to form bimetallic alloy is expected to have higher catalytic performance, better sensitivity and selectivity, relative mild operation environment as well as longer stability of electrode systems due to the synergistic effect between the metals [22,23].

Several approaches have been proposed to prepare such transition metal incorporated Au bimetallic metals with different potential applications. For example, Wang fabricated bimetallic AuCu alloy nanoparticles with engineered the composition and structure in carbon nanofibers and used it as self-supported electrode materials for electrocatalytic water splitting [24]. Shang electrodeposited AuCu alloy nanoparticles on a graphene-ionic liquid composite film and found that the AuCu nanoparticles showed high electrocatalysis to the oxidation of hydrazine [18]. Lv used a hydrothermal method and subsequent electro-anodization to prepare core/shell NiAu/Au NPs, and demonstrated it as effective catalyst with Pt-like activity for hydrogen evolution reaction [25].

In this work, we synthesize NiAu bimetallic nanostrips directly on glassy carbon electrode surface through electrochemical deposition approach in a precursor solutions involving  $\text{Ni}(\text{NO}_3)_2$  and  $\text{HAuCl}_4$  with the help of surfactant of cetyltrimethylammonium bromide (CTAB) as the stabilizer. By adjusting the molar ratio of  $\text{Ni}(\text{NO}_3)_2$  and  $\text{HAuCl}_4$  in precursor solutions, the composition and structure of AuNi bimetallic alloys can be engineered. Well-dispersed NiAu bimetallic nanostrips can be obtained when the molar ratio of the two precursors is 1:1, and it exhibits prominent electrocatalytic activities toward the oxidation of hydrazine with better performance (higher oxidation current and lower oxidation potential) than the monometallic Au and Ni material. Therefore, outstanding performance of the NiAu bimetallic nanostrips based hydrazine sensor with high detection sensitivity and selectivity, and good stability is achieved.

## 2. EXPERIMENTAL SECTION

### 2.1. Reagents and apparatus

$\text{HAuCl}_4 \cdot 3\text{H}_2\text{O}$ , glucose, ascorbic acid (AA), dopamine (DA), uric acid (UA), and

cetyltrimethylammonium bromide (CTAB) were purchased from Sigma Aldrich. Nickel nitrate, hydrogen peroxide ( $\text{H}_2\text{O}_2$ ) were obtained from Aladdin Chemical Reagent Co., Ltd. (Shanghai, China). The electrolyte solutions for electrochemical detection of hydrazine were prepared with phosphate buffer solution (0.1 M PBS: pH 8.0). All of the above chemicals were of analytical reagent grade. Deionized water was prepared with a Milli-Q water purification system.

Field-emission scanning electron microscope (FESEM, Hitachi SU-8010) equipped with energy-dispersive X-ray (EDX) was used to characterize the surface morphologies of the obtained materials. Electrodeposition, cyclic voltammetric (CV) and chronoamperometric experiments were performed on a CHI 660D electrochemical workstation with a conventional three-electrode system: a glassy carbon (GC, diameter of 3 mm) electrode with or without modifications as the working electrode, a saturated calomel electrode (SCE) as the reference electrode, and a Pt wire as the counter electrode.

## 2.2. Electrodeposition of NiAu bimetallic nanostrips

Galvanostatic technique was used to electrodeposition of NiAu bimetallic nanostrips on working electrode of GC using the above three-electrode configuration. The applied current density was set as  $3.5 \text{ mA/cm}^2$  for a certain period of time. Before electrodeposition, GC electrode was first polished with alumina powder to a mirror-like surface and subsequently rinsed with ethanol and water sequentially under sonication. The pretreated GC electrode was immersed into electrolyte solution with a total concentration of 1 mM precursor ( $\text{Ni}(\text{NO}_3)_2$  and  $\text{HAuCl}_4$ ) and 5 mM of CTAB contained. The molar ratio of  $\text{Ni}(\text{NO}_3)_2$  and  $\text{HAuCl}_4$  was adjusted to optimize the electrode performance.

## 3. RESULTS AND DISCUSSION

### 3.1. Morphological characterizations

Fig. 1 shows SEM images of the NiAu films on GC surface electrodeposited in 1 mM precursor solutions with different molar ratios of  $\text{Ni}(\text{NO}_3)_2$  and  $\text{HAuCl}_4$  involved. When the precursor contained  $\text{HAuCl}_4$  only, spherical Au nanoparticles with most diameters ranging of about 100 nm dispersed layeredly on electrode surface (Fig. 1a). However, for electrodeposition of  $\text{Ni}(\text{NO}_3)_2$  alone, a nanoporous and amorphous Ni nanostructures spread onto whole electrode (Fig. 1b). For Ni/Au precursor molar ratio of 1:1, a nearly monodispersed NiAu bimetallic nanostrips with a width of approximately 50 nm and length of 100~200 nm can be observed (Fig. 1c). With further increasing the content of Au in Ni/Au precursor solutions, as can be seen in Fig. 1d and Fig. 1e, the amount of NiAu nanostructures increase apparently, and more and more large-sized and aggregated nanoparticles appeared. Meanwhile, the morphology changed gradually from nanostrip to nanoparticles. Conversely, with further decreasing the content of Au in Ni/Au precursor solutions on the basis of molar ratio of 1:1, the size of formed NiAu nanostructures becomes smaller and both of nanoparticles and nanostrips can be separately observed from Fig. 1f and Fig. 1g. The corresponding elemental mapping images of

NiAu nanotrips prepared with Ni/Au precursor molar ratio of 1:1 is shown in Fig. 1h. Both element of Ni and Au can be clearly seen to constitute NiAu nanotrips.

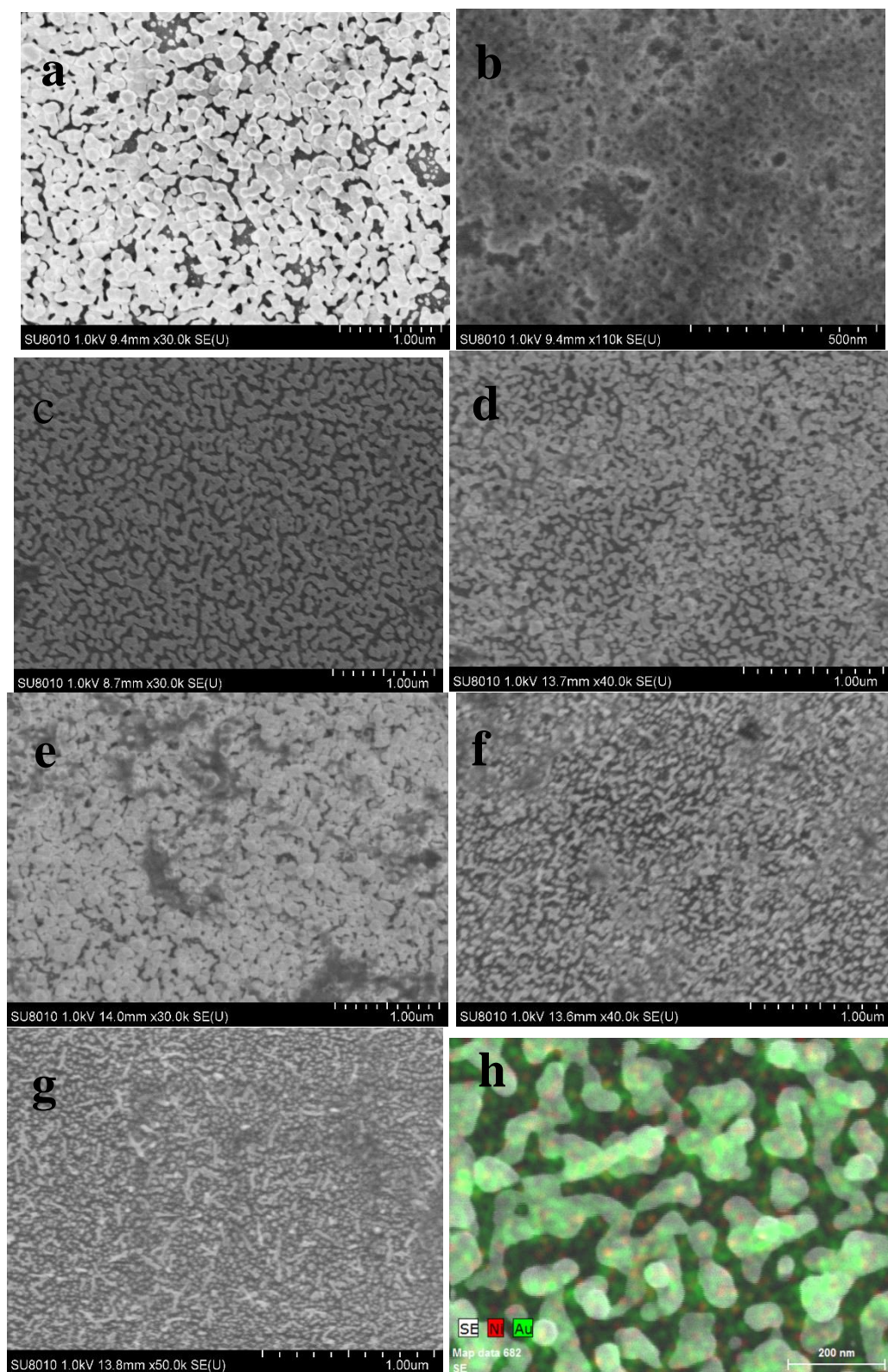


**Figure 1.** SEM images of the NiAu films on GC surface electrodeposited in 1 mM precursor solutions with different Ni/Au precursor molar ratio: (a) 0:1; (b) 1:0; (c) 1:1; (d) 1:2; (e) 1:4; (f) 2:1; (g) 4:1. (h) The corresponding elemental mapping images of NiAu nanotrips.

### 3.2. Electrocatalytic effect of NiAu bimetallic nanostrips toward hydrazine oxidation

The CV responses of 1.0 mM hydrazine on the above NiAu films modified electrodes prepared in 1 mM precursor solutions containing different Ni/Au precursor molar ratios are presented in Fig.2. As can be seen, with the increasing content of Au in Ni/Au precursor solutions, the prepared NiAu films modified electrodes show more negative peak potentials and higher peak currents toward hydrazine oxidation, indicating that Au in NiAu films plays a significant electrocatalytic effect toward hydrazine oxidation. However, a largest peak current for Ni/Au precursor molar ratio of 1:1 appeared at potential of 0.09 V, showing an optimum synergetic effect between Ni and Au in the prepared NiAu bimetallic nanostrips. Therefore, Ni/Au precursor molar ratio of 1:1 was used in the following experiment to achieve high detection sensitivity for hydrazine oxidation.

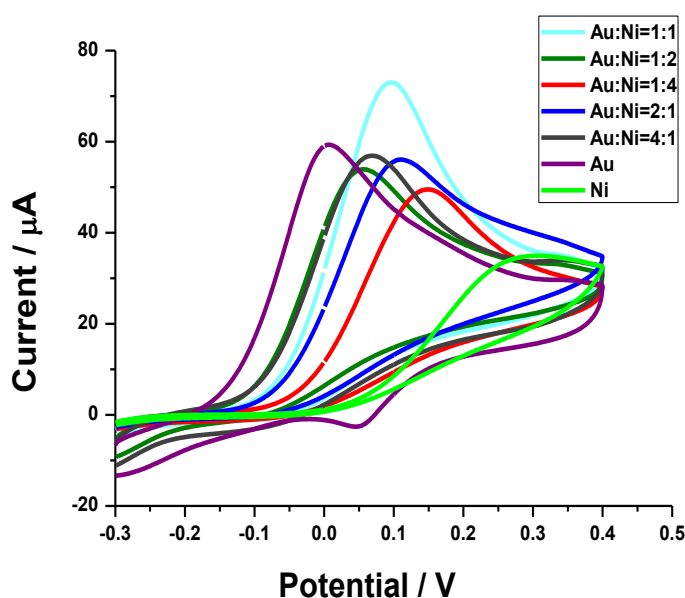


**Figure 2.** CV responses of 1.0 mM hydrazine on the above prepared NiAu films modified electrodes, 0.1 M pH 8.0 PBS was used as supporting electrolyte.

### 3.3. Optimization of experimental factors for electrochemical detection of hydrazine

#### 3.3.1 Influence of CTAB concentration

To investigate the influence of CTAB concentration on the electrodeposited NiAu nanostructures toward hydrazine oxidation, the concentration of CTAB was changed from 0 to 30 mM, while maintaining other conditions invariant. Fig. 3 shows CV responses of 1.0 mM hydrazine on NiAu bimetallic nanostrips modified electrodes prepared with different concentrations of CTAB involved. As observed, when the CTAB concentration was increased from 0 to 5 mM, an extraordinary oxidation peak of hydrazine with lower peak potential was obtained at 5 mM CTAB. However, with the further increase of CTAB concentration from 5 to 30 mM, the oxidation peak of hydrazine is decreased slowly and meanwhile the peak potential shifts positively, indicating that much larger CTAB

concentration decreased the electrocatalytic activities of the prepared NiAu films toward hydrazine oxidation. Because of the obtained higher sensitivity and lower oxidation potential, 5 mM was selected as the best CTAB concentration in the following experiment.

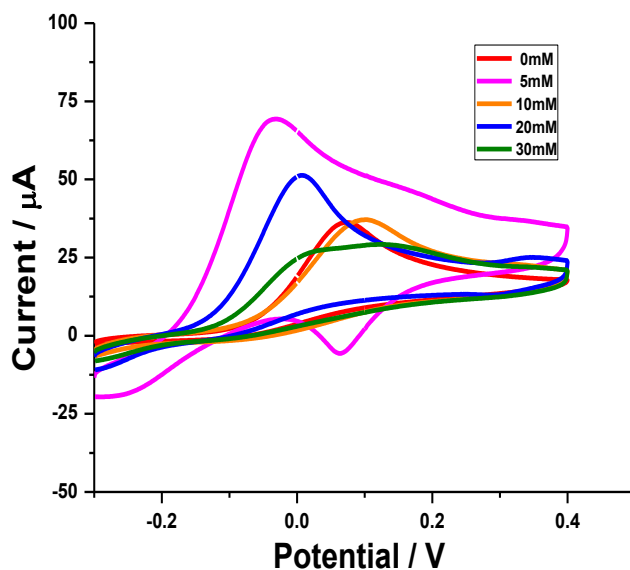


**Figure 3.** CV responses of 1.0 mM hydrazine on NiAu bimetallic nanostrips modified electrodes prepared with different concentrations of CTAB involved.

### 3.3.2 Influence of solution pH

The electrochemical response of hydrazine is affected by solution pH because of proton involved in the process of hydrazine oxidation [11,26]. Thus, we investigated the electrochemical oxidation of hydrazine in PBS solutions with different pH values, the results of which is shown in Fig.4. Obviously, the oxidation peak potentials of hydrazine shifted to negative values with the increase of pH from 5 to 9, suggesting better electrocatalytic activities of NiAu bimetallic nanostrips toward hydrazine oxidation in alkaline solutions. The electrochemical reaction of hydrazine is always described as follows [27]:  $\text{N}_2\text{H}_4 + 4\text{OH}^- = \text{N}_2 + 4\text{H}_2\text{O} + 4\text{e}^-$ . From this equation, higher concentration of  $\text{OH}^-$  can promote the reaction, thus generating more negative oxidation potential. However, the oxidation peak current enhanced gradually with the increase of pH to 8, and then decreased remarkably above pH 8, probably due to the protonation or deprotonation of hydrazine, causing a shift in the formal potential of hydrazine [28]. Considering the maximum current at pH 8 and the highest detection sensitivity, buffer solutions with pH 8 was conducted is this experiment.

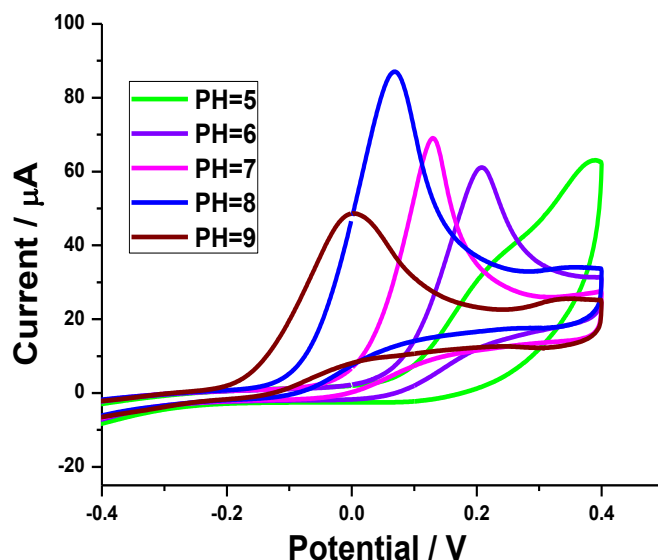


**Figure 4.** CV responses of 1.0 mM hydrazine with different pH values of PBS on NiAu bimetallic nanostrips modified electrodes.

### 3.3.3 Influence of the concentration of hydrazine

Fig. 5a presents CV responses of different concentrations of hydrazine on NiAu bimetallic nanostrips modified electrodes. With the increase of hydrazine concentration from 0 to 1 mM with an interval of 0.2 mM, the oxidation peak currents is seen to increase proportionally. The linear relationship between peaks currents and concentrations is described as  $I(\mu\text{A})=4.86824+88.84786C(\text{mM})$  with a correlation coefficient of 0.9989, revealing the NiAu bimetallic nanostrips modified electrodes responded sensitively toward the concentration change of hydrazine. Based on this results, it can be concluded that the NiAu bimetallic nanostrips shows perspective for electrochemical detection of hydrazine.

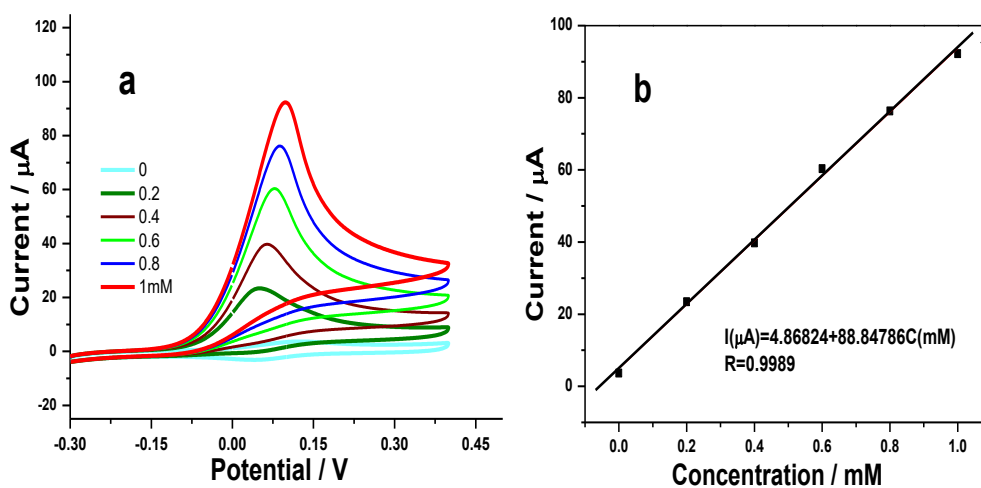


**Figure 5.** CV responses of different concentrations of hydrazine on NiAu bimetallic nanostrips modified electrodes (a) and the corresponding linear relationship between current and concentration (b).

### 3.4. Amperometric detection of hydrazine

Under optimized conditions, 1 mM precursor solutions containing 5 mM CTAB and Ni/Au molar ratio of 1:1 was used to electrodeposite NiAu bimetallic nanostrips. At a constant potential of 0.06 V, the resultant electrode is dipped into 0.1 M pH 8.0 PBS solution and the amperometric response is recorded. After 800 s until a constantly blank current obtained, a certain concentration of hydrazine is added for an interval of 50 s to obtain the amperometric response. As shown in Fig.6a, well-defined amperometric currents increasing stepwise with the amount of H<sub>2</sub>O<sub>2</sub> are obtained. The response time is less than 3 s, according to the definition that the time required to reach 90% steady-state current from the onset addition, revealing that NiAu bimetallic nanostrips respond effectively and rapidly toward the oxidation of hydrazine. Calibration plot between the current response and the concentration of hydrazine is presented in Fig. 6b. A good linear response range for 0.5~1665  $\mu\text{M}$  is obtained. The corresponding linear regression equation is expressed as  $I(\mu\text{A})=0.68531+0.07569C(\mu\text{M})$  with a correlation coefficient of 0.9974. From the slope of this calibration plot, the detection limit and detection sensitivity are deduced to be 0.1  $\mu\text{M}$  (signal-to-noise ratio of 3) and 1071  $\mu\text{A mM}^{-1} \text{cm}^{-2}$  or 75.69  $\mu\text{A mM}^{-1}$ , respectively.

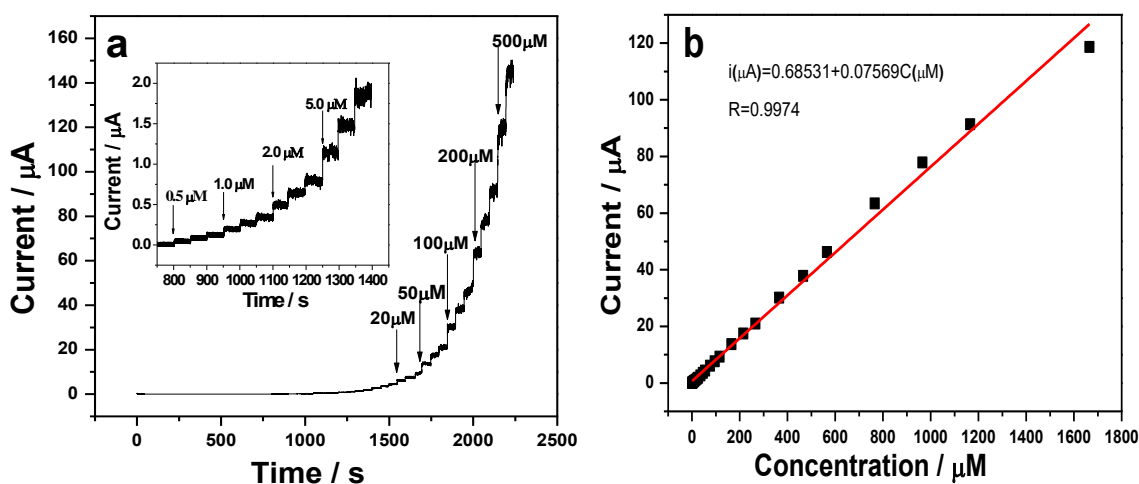


**Figure 6.** (a) Amperometric responses of NiAu bimetallic nanostrips modified electrode (holding at 0.06 V) upon addition of hydrazine to increasing concentrations; (b) The calibration curve with the data obtained from fig.6a.

The comparison of the performance of the developed NiAu bimetallic nanostrips with other materials for hydrazine detection is listed in Table 1. As observed, the determination results obtained at NiAu bimetallic nanostrips including the response time, detection sensitivity, linear range and LOD are among the top list of various nanomaterials. For example, the detection sensitivity is obviously higher than other nanomaterials displayed in table 1, such as AuCu alloy nanoparticles-graphene-ionic liquid composite (AuCu-EGN-IL, 56.7  $\mu\text{A mM}^{-1}$ ) [18], silver dendritic structures (20.81  $\mu\text{A mM}^{-1} \text{cm}^{-2}$ ) [29], hierarchical flower-like cobalt on petalage-like graphene hybrid microstructures (Co-GE, 562.5  $\mu\text{A mM}^{-1} \text{cm}^{-2}$ ) [30], graphene nanoflakes (28  $\mu\text{A mM}^{-1}$ ) [31], MnO<sub>2</sub>/graphene oxide composite nanosheets (1007  $\mu\text{A mM}^{-1} \text{cm}^{-2}$ ) [32] and Mn(II)-complex multi-wall carbon nanotubes (Mn(II)-complex/MWNTs, 38  $\mu\text{A mM}^{-1}$ ) [33]. Based on these results, it can be concluded that the developed

NiAu bimetallic nanostrips exhibits outstanding performance for electrochemical sensing of hydrazine.

**Table 1.** Comparison of NiAu bimetallic nanostrips with with other materials for hydrazine detection.

Electrode materials	Response time (s)	Sensitivity	Linear range ( $\mu\text{M}$ )	LOD ( $\mu\text{M}$ )	Ref.
AuCu-EGN-IL	-	$56.7 \mu\text{A mM}^{-1}$	0.2~110	0.1	18
silver dendrites	<5	$20.81 \mu\text{A mM}^{-1} \text{ cm}^{-2}$	100~1700	0.5	29
Co-GE	2-3	$562.5 \mu\text{A mM}^{-1} \text{ cm}^{-2}$	0.25~370 370~2200	0.1	30
graphene nanoflakes	<3	$28 \mu\text{A mM}^{-1}$	0.5~7.5	0.3	31
$\text{MnO}_2$ /graphene oxide	-	$1007 \mu\text{A mM}^{-1} \text{ cm}^{-2}$	3~1120	0.16	32
Mn(II)-complex/MWNTs	-	$38 \mu\text{A mM}^{-1}$	1~1050	0.5	33
NiAu bimetallic nanostrips	<3	$1071 \mu\text{A mM}^{-1} \text{ cm}^{-2}$ or $75.69 \mu\text{A mM}^{-1}$	0.5~1665	0.1	This work

The reproducibility of NiAu bimetallic nanostrips modified electrodes toward hydrazine detection was investigated from its current response to  $50 \mu\text{M}$  hydrazine using six electrodes prepared separately under the same conditions. The relative standard deviation (RSD) was found to be 5.6%, indicating an acceptable reproducibility of the sensor preparation. The repeatability was examined by steady-state current response of  $50 \mu\text{M}$  hydrazine for eight successive measurement. The obtained RSD was only 3.5%, suggesting excellent repeatability of the NiAu bimetallic nanostrips electrode. The storage stability was determined by monitoring the current response periodically and the oxidation current retained 86% of the initial value after intermittent usage for one month.

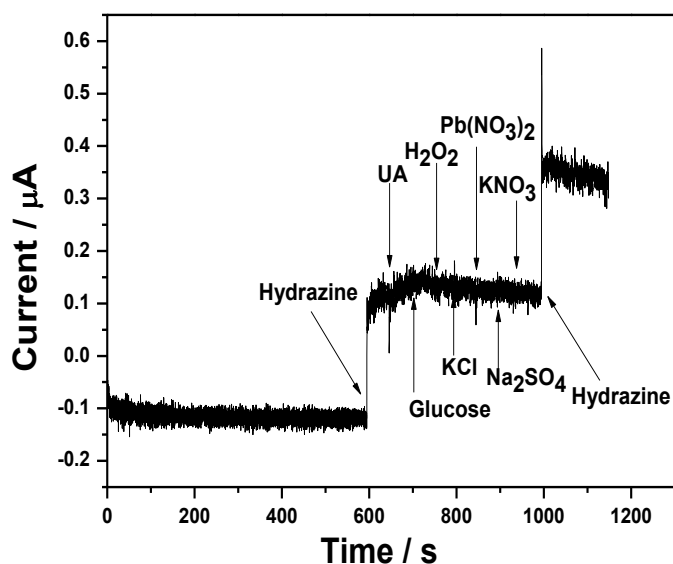


**Figure 7.** Amperometric responses of the NiAu bimetallic nanostrips modified electrode to successive additions of  $5 \mu\text{M}$  Hydrazine,  $0.5 \text{ mM}$  UA, glucose,  $\text{H}_2\text{O}_2$ , KCl,  $\text{Pb}(\text{NO}_3)_2$ ,  $\text{Na}_2\text{SO}_4$ ,  $\text{KNO}_3$  in  $0.1 \text{ M}$  pH 8.0 PBS at  $0.06 \text{ V}$ .

The selectivity of the present method was studied for hydrazine detection in presence of

various interfering species. The amperometric response for the addition of 5  $\mu\text{M}$  hydrazine was recorded followed by the added hundredfold excess concentrations of the possible interfering species. Fig. 7 exhibits responses of the NiAu bimetallic nanostrips modified electrode to successive additions of 5  $\mu\text{M}$  hydrazine, 0.5 mM UA, glucose,  $\text{H}_2\text{O}_2$ , KCl,  $\text{Pb}(\text{NO}_3)_2$ ,  $\text{Na}_2\text{SO}_4$  and  $\text{KNO}_3$  in 0.1 M pH 8.0 PBS at 0.06 V. The change in the current response is negligible upon the addition of interfering species compared with that of hydrazine, indicating a good selectivity of the present method for hydrazine detection.

### 3.5. Real sample analysis

In order to verify the reliability of the proposed method, two different water samples including tap water and river water spiked with known concentrations of hydrazine are prepared. The amperometric current response of these samples at NiAu bimetallic nanostrips modified electrode was measured, and the corresponding concentration of determined hydrazine is predicted from the calibration curve. The analytical results were displayed in Table 2. Obviously, the determined results are consistent with the spiked values, and the obtained recovery is satisfactory, indicating that the present method is feasible for determination of hydrazine in real samples.

**Table 1.** Amperometric determination of hydrazine spiked in tap water and river water samples (n=4).

Water samples	Spiked ( $\mu\text{M}$ )	Determined ( $\mu\text{M}$ )	RSD(%)	Recovery (%)
Tap water	10	9.7	2.8	97
River water	20	20.4	3.4	102

## 4. CONCLUSIONS

In summary, we successfully synthesized NiAu bimetallic nanostrips directly on electrode surface through electrochemical deposition approach in 1 mM precursor solutions with Ni/Au molar ratio of 1:1 with the help of surfactant CTAB. The obtained NiAu bimetallic nanostrips showed good electrocatalytic activities toward hydrazine oxidation and it was used for electrochemical detection of hydrazine. A good performance, including quick response (below 3 s), wide linear response range of 0.5 to 1665  $\mu\text{M}$ , low detection limit of 0.1  $\mu\text{M}$ , high detection sensitivity of 1071  $\mu\text{A mM}^{-1} \text{cm}^{-2}$  and good reproducibility and stability was obtained. The developed method was highly selective for hydrazine determination in presence of hundredfold of common ions and organic interferents. Herein, the simple electrodeposition method accompanied by surfactant as stabilizer may pave the way for the synthesis of new, nanoscale metal or multimetal alloy materials with unique morphology and properties, which can be used to design novel electrochemical sensors.

## ACKNOWLEDGMENTS

This work was supported by the Grants from the National Natural Science Foundation of China (21105002, U1704135), the Technology Development Plan Project for Anyang City (21) and and the Innovative Foundation for the College students of Anyang Normal University (ASCX/2018-Z039).

## References

1. Y.W. Lee, M. Kim, Y. Kim, S.W. Kang, J.-H. Lee and S.W. Han, *J. Phys. Chem. C*, 114 (2010) 7689.
2. L. Aldous and R.G. Compton, *ChemPhysChem*, 12 (2011) 1280.
3. Q. Wan, Y. Liu, Z. Wang, W. Wei, B. Li, J. Zou and N. Yang, *Electrochem. Commun.*, 29 (2013) 29.
4. X.B. Ji, C.E. Banks, W. Xi, S.J. Wilkins and R.G. Compton, *J. Phys. Chem. B*, 110 (2006) 22306.
5. S.M. Golabi and H.R. Zare, *J. Electroanal. Chem.*, 465 (1999) 168.
6. X. Yan, F. Meng, S. Cui, J. Liu, J. Gu and Z. Zou, *J. Electroanal. Chem.*, 661 (2011) 44.
7. Y.-Y. Liu, I. Schmeltz and D. Hoffmann, *Anal. Chem.*, 46 (1974) 885.
8. M. George, K.S. Nagaraja and N. Balasubramanian, *Talanta*, 75 (2008) 27.
9. J.C. Huang, C.X. Zhang and Z.J. Zhang, *Fresenius J. Anal. Chem.*, 363 (1999) 126.
10. W. Gao, J. Xi, Y. Chen, S. Xiao, Y. Lin and Y. Chen, *Anal. Methods*, 4 (2012) 3836
11. M. Mazloun-Ardakani and A. Khoshroo, *Electrochim. Acta*, 103 (2013) 77.
12. F. Li, Y. Ji, S. Wang, S. Li and Y. Chen, *Electrochim. Acta*, 176 (2015) 125.
13. F. Zhang, L. Zhang, J. Xing, Y. Tang, Y. Chen, Y. Zhou, T. Lu, and X. Xia, *ChemPlusChem*, 77 (2012) 914.
14. J. Deng, S. Deng and Y. Liu, *Int. J. Electrochem. Sci.*, 13 (2018) 3566.
15. D.H. Deng, Y.Q. Hao, S.L. Yang, Q.Y. Han, L. Liu, Y.R. Xiang, F.B. Tu and N. Xia, *Sens. Actuators B*, 286 (2019) 415.
16. N. Xia, X. Wang, J. Yu, Y.Y. Wu, S.C. Cheng, Y. Xing and L. Liu, *Sens. Actuators B*, 239 (2016) 834.
17. N. Xia, X. Wang, B.B. Zhou, Y.Y. Wu, W.H. Mao and L. Liu, *ACS Appl. Mat. Interfaces*, 8 (2016) 19303.
18. L. Shang, F. Zhao and B. Zeng, *Electroanalysis*, 24 (2012) 2380.
19. C. Y. Tai, J.L. Chang, J.F. Lee, T.S. Chan and J.M. Zen, *Electrochim. Acta*, 56 (2011) 3115.
20. L. Qin, L. He, J. Zhao, B. Zhao, Y. Yin and Y. Yang, *Sens. Actuators B* 240 (2017) 779.
21. T. Sakamoto, K. Asazawa, J. Sanabria-Chinchilla, U. Martinez, B. Halevi, P. Atanassov, P. Strasser and H. Tanaka, *J. Power Sources*, 247 (2014) 605.
22. B.D. Chandler, C.G. Long, J.D. Gilbertson, C.J. Pursell, G. Vijayaraghavan, and K.J. Stevenson, *J. Phys. Chem. C*, 114 (2010) 11498.
23. A.B. Vysakh, C.L. Babu, and C.P. Vinod, *J. Phys. Chem. C*, 119 (2015) 8138.
24. J. Wang, H. Zhu, D. Yu, J.W. Chen, J.D. Chen, M. Zhang, L.N. Wang, and M.L. Du, *ACS Appl. Mater. Interfaces*, 9 (2017) 19756.
25. H. Lv, Z. Xi, Z. Chen, S. Guo, Y. Yu, W. Zhu, Q. Li, X. Zhang, M. Pan, G. Lu, S. Mu, and S. Sun, *J. Am. Chem. Soc.*, 137 (2015) 5859.
26. B. Haghghi, H. Hamidi and S. Bozorgzadeh, *Anal. Bioanal. Chem.*, 398 (2010) 1411.
27. Q. Yi and W. Yu, *J. Electroanal. Chem.*, 633 (2009) 159.
28. M.A. Kamyabi, O. Narimani and H.H. Monfared, *J. Electroanal. Chem.*, 644 (2010) 67.
29. R. Sivasubramanian and M.V. Sangaranarayanan, *Sens. Actuators B*, 213 (2015) 92.
30. Y. He, J. Zheng and S. Dong, *Analyst*, 137 (2012) 4841.
31. S. Mutyala and J. Mathiyarasu, *Sens. Actuators B* 210 (2015) 692.
32. J. Lei, X. Lu, W. Wang, X. Bian, Y. Xue, C. Wang and L. Li, *RSC Advances*, 2 (2012) 2541.
33. M.A. Kamyabi, O. Narimani and H.H. Monfared, *J. Electroanal. Chem.*, 644 (2010) 67.